

Accepted for publication in The Astronomical Journal

## An IR–Selected Galaxy Cluster at $z = 1.27^1$

S.A. Stanford

Institute of Geophysics and Planetary Physics, Lawrence Livermore National Laboratory,  
Livermore, CA 94550

Richard Elston<sup>2</sup>

Department of Astronomy, University of Florida, Gainesville, FL 32611

Peter R. Eisenhardt<sup>2</sup>

Jet Propulsion Laboratory, California Institute of Technology, Pasadena, CA 91109

Hyron Spinrad, Daniel Stern

Astronomy Department, University of California, Berkeley, CA 94720

and

Arjun Dey

National Optical Astronomy Observatories<sup>3</sup>, Tucson, AZ 85726

### ABSTRACT

We report the discovery of a galaxy cluster at  $z = 1.27$ . ClG J0848+4453 was found in a near-IR field survey as a high density region of objects with very red  $J - K$  colors. Optical spectroscopy of a limited number of  $24 \lesssim R \lesssim 25$  objects in the area shows that 6 galaxies within a 90 arcsec ( $0.49 h_{100}^{-1}$  Mpc,  $q_0 = 0.1$ ) diameter region lie at  $z = 1.273 \pm 0.002$ . Most of these 6 member galaxies have broad-band colors consistent with the expected spectral energy

---

<sup>1</sup>Based in part on observations obtained at the W.M. Keck Observatory

<sup>2</sup>Visiting Astronomer, Kitt Peak National Observatory, National Optical Astronomy Observatories, which is operated by the Association of Universities for Research in Astronomy, Inc., under cooperative agreement with the National Science Foundation.

<sup>3</sup>The National Optical Astronomy Observatories are operated by the Association of Universities for Research in Astronomy, Inc., under cooperative agreement with the National Science Foundation.

distribution of a passively-evolving elliptical galaxy formed at high redshift. An additional 2 galaxies located  $\sim 2$  arcmin from the cluster center are also at  $z = 1.27$ . Using all 8 of these spectroscopic members, we estimate the velocity dispersion  $\sigma = 700 \pm 180 \text{ km s}^{-1}$ , which is similar to that of Abell richness class  $R = 1$  clusters in the present epoch. A deep Rosat/PSPC archival observation detects X-ray emission at the  $5 \sigma$  level coincident with the nominal cluster center. Assuming that the X-ray flux is emitted by hot gas trapped in the potential well of a collapsed system (no AGN are known to exist in the area), the resulting X-ray luminosity in the rest frame 0.1–2.4 keV band of  $L_x = 1.5 \times 10^{44} \text{ ergs s}^{-1}$  suggests the presence of a moderately large mass. ClG J0848+4453 is the highest redshift cluster found without targetting a central active galaxy.

*Subject headings:* galaxies: clusters — galaxies: evolution — galaxies: formation

## 1. Introduction

The existence of massive collapsed objects, such as rich galaxy clusters, at high redshift provides a challenge for theories of cosmic structure formation (Press & Schechter 1974). Numerical simulations based on hierarchical clustering models such as cold dark matter (CDM) offer useful predictions of the evolution of the cluster number density with cosmic time (*e.g.* Cen & Ostriker 1994a; Eke, Cole, & Frenk 1996; Viana & Liddle 1996; Bahcall, Fan, & Cen 1997). The rate at which clusters form depends strongly on  $\Omega_0$ , and weakly on  $\Lambda$  and the initial power spectrum. CDM predicts that the cluster population evolves rapidly for  $\Omega_0 = 1$ , and very slowly for a low-density universe (*e.g.* Peebles, Daly, & Juszkievicz 1989; Evrard 1989). So far a census of high redshift clusters sufficiently complete for such model tests has been difficult to assemble.

In addition to their utility in large-scale structure studies, high redshift galaxy clusters provide important tools in the study of galaxy formation and evolution. The galaxy populations of rich cluster cores up to at least  $z \sim 1$  tend to be dominated by massive ellipticals, which are good probes of galaxy evolution because their stellar populations appear to be relatively simple. Ellipticals in present-epoch clusters form a homogeneous population (Bower, Lacey, & Ellis 1992; De Propris et al. 1997), which has been largely quiescent since at least  $z \sim 1$  (Aragón-Salamanca et al. 1993; Lubin 1996; Ellis et al. 1997; Stanford, Eisenhardt, & Dickinson 1998, hereinafter SED98). The nature of elliptical galaxy formation at even higher redshifts probably depends strongly on the importance of merging in assembling the stellar mass. Beyond  $z \sim 1$  in cosmologically flat CDM models,

the amount of merging occurring within the prior  $\sim 1$  Gyr is large and could seriously inflate the locus of early-type galaxy colors due to interaction-induced starbursts (Kauffmann 1996). On the other hand, models in which ellipticals formed by a monolithic collapse at high- $z$  (e.g. Eggen, Lynden-Bell, & Sandage 1962) predict a tight color-magnitude relation out to at least  $z \sim 2$  for reasonable cosmologies. Thus, the identification of clusters at  $z > 1$  and the characterization of their galaxy populations provides a powerful means of testing elliptical galaxy formation theories.

Finding high redshift clusters is difficult. The field galaxy population overwhelms traditional searches for two-dimensional overdensities in the optical. Most searches have targeted high redshift radio galaxies and quasars under the assumption that such massive objects may be signposts of early collapse and the existence of massive dark matter halos. Several probable  $z > 1$  clusters have been found using this method, including 3C 324 at  $z = 1.20$  (Dickinson 1995) and 53W002 at  $z = 2.39$  (Pascarelle et al. 1996). Many other more tentative candidates have been published as well, in which claims of cluster identification often are based only on  $\lesssim 3$  common redshifts, including the AGN. 3C 324 is the highest redshift example of a massive cluster which has strong evidence of both a large number of known members, based on extensive optical spectroscopy, *and* of a deep potential well, in the form of extended X-ray emission (Dickinson 1996).

An emerging method of finding  $z > 1$  cluster candidates is deep near-IR sky surveys. Because their near-IR light is dominated by the light of evolved giant stars, the  $J - K$  colors of nearly all galaxies are simple functions of redshift out to  $z \sim 2$ . Though still constrained by the relatively small size of the available arrays, near-IR imaging surveys soon may offer a viable alternative to X-ray searches, which at present are limited to the detection of only the most massive clusters at  $z \sim 1$ . If the strong redshift evolution in clusters predicted by CDM is correct, then the more interesting mass regime of collapsed objects at  $z > 1$  may be that of poor clusters not yet entirely virialized. Near-IR imaging surveys may be able to provide a cluster sample at very high redshift complete to a relatively low mass limit. We describe here the discovery of one  $z > 1$  cluster which resulted from a near-IR field survey. Except where noted, the assumed cosmology is  $H_0 = 65 \text{ km s}^{-1} \text{ Mpc}^{-1}$  and  $q_0 = 0.1$ .

## 2. Observations

### 2.1. Survey Imaging

Elston, Eisenhardt, & Stanford (1997, hereinafter EES) have recently completed a *BRIzJK* field survey designed to cover  $\sim 100 \text{ arcmin}^2$  over four areas of high galactic

latitude sky down to  $K \sim 22$ . The observations were carried out at the 4 m telescope of the Kitt Peak National Observatory. Optical imaging was obtained with the PFCCD/T2KB, which gives  $0.48''$  pixels over a  $16'$  field. The IR imaging was obtained with IRIM, in which a NICMOS3 HgCdTe array provides  $0.6''$  pixels over a  $\sim 2.5'$  field. Details of the observing and reductions are given in EES. The *BRJK* survey images were coaligned and convolved to the same effective PSF of  $\text{FWHM} \approx 1.5''$ . Calibrations of the optical and IR images onto the Landolt and CIT systems were obtained using observations of Landolt and UKIRT standard stars, respectively. The *I* and *z* survey data are not considered here due to problems with fringing and photometric calibration.

A catalog of objects within the  $28 \text{ arcmin}^2$  Lynx portion of the EES survey was obtained from the *K* image using FOCAS (Valdes 1982), as revised by Adelberger (1996). The image was smoothed with a  $2''.4 \times 2''.4$  kernel, and object detection was performed down to an isophotal level corresponding to  $4 \sigma$  above sky, with a minimum object size of  $3.2 \text{ arcsec}^2$ . Photometry was obtained through  $2''$  diameter apertures using this catalog on the *BRJK* images; the  $4 \sigma$  limit in the *K* band is 21.4. A sample of very red objects was then selected using a  $J - K \gtrsim 1.9$  criterion to search for  $z > 1$  galaxies. Serendipitously, a large overdensity of these very red objects appeared in a small region in the Lynx survey field. Of the 103 objects with  $J - K \gtrsim 1.9$  down to  $K = 21.0$  in the entire  $28 \text{ arcmin}^2$  field, 25 fall within a circular area of radius  $\lesssim 45''$ . In this region, the density of the very red objects (hereinafter referred to as a spatially compact group, or SCG) is  $13.6 \text{ arcmin}^{-2}$ , in contrast to  $2.8 \text{ arcmin}^{-2}$  over the rest of the  $28 \text{ arcmin}^2$  of the Lynx survey field.

Additional *JHK* imaging of a smaller area at the SCG was obtained at the KPNO 4m telescope with IRIM in February 1997. After standard reductions, the new *JK* imaging was combined with that from the field survey in the SCG area to produce deep *JK* images, which we use in the remainder of this paper in place of the survey *JK* imaging. The new data were obtained to improve the photometry of the objects in a  $9 \text{ arcmin}^2$  area at the SCG. The summed images have  $4\sigma$  limits of  $K = 21.7$ ,  $H = 22.4$  and  $J = 23.1$  in  $2.4 \text{ arcsec}$  diameter apertures. Figure 1 (plate X) shows greyscale images in the *K* and *R* bands of the SCG, with the  $J - K \gtrsim 1.9$  objects highlighted.

## 2.2. Keck Spectroscopy

Based on the discovery of the SCG, we proceeded to obtain optical spectroscopy in a limited area of the Lynx survey field. Objects were selected using the  $J - K$  color and the *R* magnitude, and are listed in Table 1. We prepared a slitmask including slitlets for 14 objects with  $J - K \gtrsim 1.9$ , 6 of which are within the SCG. Five other objects outside

the SCG were included so as to fill out the mask. The slits had widths of 1.5 arcsec and minimum lengths of 10 arcsec. The slitmask was used with the Low Resolution Imaging Spectrograph (LRIS; Oke et al. 1995) on the 10 m Keck II telescope on 03-04 February 1997 UT to obtain deep spectroscopy. We used the 400 l mm<sup>-1</sup> grating, which is blazed at 8500 Å, to cover a nominal wavelength range of 6000 to 9700 Å, depending on the position of a slit in the mask. The dispersion of  $\sim 1.8$  Å pixel<sup>-1</sup> resulted in a spectral resolution of  $\sim 9$  Å, which is the FWHM of the emission lines in the arc lamp spectra. We obtained  $6 \times 1800$  s exposures with this setup in photometric conditions with subarcsec seeing. Objects were shifted along the long axis of the slits between exposures to enable better sky subtraction.

The slitmask data were separated into 19 individual spectra and then reduced using standard longslit techniques. The 6 exposures for each object/slitlet were reduced separately and then coadded for each night separately. The spectra were reduced both without and with a fringe correction; the former tends to yield higher quality object spectra at the shorter wavelengths, while the latter is necessary at the longer wavelengths. Wavelength calibration was obtained from arc lamp exposures taken immediately after the object exposures. A relative flux calibration was obtained from a longslit observation of the standard stars HZ 44 and G191B2B with the 400 l mm<sup>-1</sup> grating. While these spectra do not straightforwardly yield an absolute flux calibration of the slit mask data, the relative calibration of the spectral shapes should be accurate. One-dimensional spectra were extracted for each of the 19 objects in the 2 sets of summed images from the 2 observing nights.

### 2.3. Rosat Archive

A search of the Rosat Archive resulted in the discovery of a deep PSPC observation which includes the SCG within the on-axis field of diameter  $\sim 40'$ . A 64 ksec PSPC observation was obtained in two exposures (sequence rp900009p) on two dates in 1991 centered at  $\alpha = 08^h 49^m 12^s.0$ ,  $\delta = +44^\circ 50' 24''$  (J2000), which is  $\approx 7.5$  arcmin from the center of the SCG. We obtained these exposures from the Rosat Archive and processed them into two images using all available channels. The two reduced images were then summed, after a very small spatial shift to achieve coalignment, to produce a single image of the field in the 0.1–2.4 keV band.

## 3. Results

### 3.1. Optical Spectroscopy

Spectral features characteristic of galaxies were identified in all but 2 of the 19 spectra; one object (#109, the bluest in  $J - K$ ) proved to be a star and another (#262,  $R = 25.4$ ) was too faint to classify. We calculated redshifts where possible from well-known rest frame stellar absorption and emission lines such as Ca II H+K and [O II] $\lambda$ 3727; these are given in Table 1. All 6 of the targeted objects in the SCG were found to lie at approximately the same redshift, with an average value of 1.273. Two more galaxies at distances of  $\sim 2$  arcmin from the SCG center lie at  $z = 1.27$  as well. Another object, #148, was found to have the same redshift, but lies nearly 4 arcminutes from the SCG center. We will assume that it is too far away to be considered part of the apparent cluster. A histogram of the 18 redshifts determined from our spectroscopy is shown in Figure 2. Of the 14 objects with  $J - K \gtrsim 1.9$ , only #82 has  $z < 1$ . This high success rate lends credence to the model-based prediction that a red  $J - K$  color is a reliable way to identify high redshift galaxies.

The 8 spectroscopic members are listed in Table 2, which gives the identified spectral features in each case. Spectra of most of the members show absorption lines (Ca II H+K, MgI  $\lambda$ 2852 and  $\lambda$ 3830, and MgII  $\lambda$ 2800) and spectral breaks (D4000, B2900, B3260 [Hamilton 1985, Fanelli et al. 1990]) similar to present-epoch ellipticals. An example, the 3 hour summed spectrum of the galaxy brightest at  $R$  (#65), is shown in Figure 3. Two of the  $z = 1.27$  galaxies have significant [O II] emission; these are also relatively blue in  $R - K$ . To better determine the redshifts of the 8 candidate cluster members, we used the fourier quotient technique as implemented in the FXCOR task of IRAF. The 6 red members were cross-correlated with a spectrum of M32, and the two emission-line galaxies with an Sc template (Kinney et al. 1996). The resulting redshifts, along with their uncertainties, are listed in Table 2. Based on these 8 members, we adopt a nominal center for 0848+4453 at  $\alpha = 8^h 48^m 34^s.6$ ,  $\delta = +44^\circ 53' 42''$  (J2000).

We have calculated an estimate of the line of sight velocity dispersion in the candidate cluster, which should be treated with caution due to the small number of members. Following the recommendation of Beers, Flynn, & Gebhardt (1990) for a very small data set, we used the “gapper” method, as implemented by their ROSTAT package, to calculate  $\sigma = 740 \pm 190 \text{ km s}^{-1}$  in the cluster rest frame. A somewhat more intuitive, if less robust, estimate may be obtained from the classical standard deviation estimator. Assuming an underlying Gaussian for the galaxy velocities, we find that  $\sigma = 700 \pm 180 \text{ km s}^{-1}$ . These dispersion estimates approximately correspond to the median value for Abell richness class  $R = 1$  (Zabludoff et al. 1993). If we assume an isothermal gas sphere model, we can calculate the mass contained within a given radius from the velocity dispersion. Using  $\sigma = 700 \text{ km s}^{-1}$ , we find that the mass within the Abell radius,  $1.5h_{100}^{-1} \text{ Mpc}$ , is

$M = 3.5_{-1.5}^{+2.0} \times 10^{14} h_{100}^{-1} M_{\odot}$ . We have chosen to use the Abell radius for mass estimates because it is similar to the virial radius often used in theoretical calculations.

### 3.2. Optical–IR Photometry

We have obtained more accurate photometry for the objects in the SCG by making use of the more recent February 1997 imaging data set. Object detection (as well as the subsequent photometry) on the  $K$  image of the SCG was performed with FOCAS using parameters similar to those of the initial catalog described in §2.1. Photometry of objects in the resulting catalog was obtained on the  $BRJHK$  images in  $2.4''$  diameter apertures. The Galactic  $E(B - V) \approx 0.04$  toward the Lynx field is small, so we have not applied an extinction correction to our photometry.  $BRJHK$  photometry of all 8 spectroscopic members within the SCG is given in Table 3. Objects #95 and 181 lie outside the area of the February 1997 imaging so only  $BRJK$  magnitudes based on the survey imaging (EES) are available. The errors in Table 3 do not include systematics due to the uncertainties in e.g. the zeropoints and PSF matching. We estimate the quadrature sum of the systematic errors in the photometry to be  $\sim 0.05$  for the IR colors, and  $\sim 0.04$  for the optical- $K$  colors.

The  $J - K$  and  $R - K$  vs  $K$  color–magnitude diagrams for all objects in a  $9 \text{ arcmin}^2$  area around the SCG are shown in Figure 4. Also plotted in both panels of Figure 4 are estimates of the no–evolution color–magnitude locus for early–type galaxies. The dashed lines were calculated as described in SED98 using photometry of early–type galaxies from a  $UBVRIzJHK$  dataset covering the central  $\sim 1 \text{ Mpc}$  of the Coma cluster (Eisenhardt et al. 1997). This data set enables us to determine, by interpolation, the colors that Coma galaxies would appear to have if the cluster could be placed at  $z = 1.27$  and observed through the  $RJK$  filters used on 0848+4453. Most of the objects within the SCG at  $K < 20$  are significantly bluer than present–epoch cluster ellipticals in  $R - K$ , and similar or slightly bluer in  $J - K$ . Because the uncertainty in the zeropoint of the Coma no–evolution prediction is similar to the amount of expected color evolution in  $J - K$ , we do not find strong evidence for passive evolution of the cluster galaxies in the observed  $J - K$  color.

The colors of most of the spectroscopic members (the encircled points in Figure 4) are broadly consistent with the predictions of a “standard” BC97 elliptical galaxy model for  $z = 1.27$ . By standard we mean the case of passive evolution of a 1 Gyr burst stellar population with solar metallicity formed at  $z = 5$  for  $h = 0.65$ ,  $q_0 = 0.1$ . Such a model predicts  $R - K = 6.0$  and  $J - K = 1.9$  at  $z = 1.27$  for a galaxy age of 3.25 Gyr. It is noteworthy that the same “standard” passive–evolution model was also found to provide a reasonable fit to the average optical–IR colors of early–type galaxies in a large sample of

clusters at  $0.3 < z < 0.9$  (SED98). For  $z_f < 3$  in our standard BC97 model, the predicted  $R - K$  becomes uncomfortably blue with respect to the colors of the known  $z = 1.27$  galaxies (except for #237; see below). Ages less than  $\sim 3$  Gyr for the stellar populations could be accommodated if the mean metallicity were greater than solar. Also, we have made no attempt to correct the colors for extinction due to dust internal to the galaxies. If this is large, then the true colors of the cluster galaxies would be bluer than our measured values, resulting in a better fit to models with  $z_f < 3$ .

The 6 spectroscopic members in the central area of the cluster broadly fall into two groups, the red objects (#65, 70, 108, 135, 142), and the lone blue object, #237. In Figure 5, we have plotted broad-band spectral energy distributions (s.e.d.) of the two groups constructed from their observed  $BRJHK$  band photometry. The red objects were normalized at  $K$  and averaged together, without weighting. Also shown in Fig. 5 are two BC97 models. The “standard” elliptical model described above provides a reasonably good fit to the average s.e.d. of the red objects, except at rest frame  $\sim 1900\text{\AA}$ . To better fit #237, a second model is shown, which combines a 1 Gyr burst with a 1% (by mass) burst added at an age of 2.25 Gyr, *i.e.* the recent starburst has an age of 1 Gyr at the 3.25 Gyr age of the composite model. In both cases, the models are scaled so as to match the flux densities at the reddest (observed  $K$ ) band.

Using our standard BC97 elliptical model and our assumed cosmology, we calculated the absolute magnitudes in the rest frame  $V$  band from the observed frame  $J$  for the cluster members; these are listed in Table 3. The  $M_V$  range from  $-23.5$ , about 2 magnitudes brighter than  $L^*$  in present-epoch clusters (Colless 1989), to  $-21.7$  for the bluest galaxy. The BC97 model predicts  $\approx 1.3$  magnitudes of luminosity evolution in  $M_V$  from  $z = 1.27$  to  $z = 0$  in our assumed cosmology, suggesting that the most luminous of the cluster members would evolve into  $\sim 2 \times L^*$  ellipticals in the present epoch.

### 3.3. X-ray Imaging

The summed PSPC image yields a detection of  $89 \pm 19$  counts in a 60 arcsec radius region centered on the nominal center of the spectroscopically identified members. The centroid of the X-ray counts in this region lies at  $\alpha = 8^h 48^m 35^s.1$ ,  $\delta = +44^\circ 53' 49''$  (J2000), which is within  $\sim 9''$  of the nominal optical cluster center. The flux in the observed 0.1–2.4 keV band is  $1.8 \times 10^{-14}$  ergs s $^{-1}$  cm $^{-2}$  in a 2 arcmin diameter region at the cluster. The origin of the X-ray flux could be several types of sources, such as lower-redshift galaxy groups, AGN within the SCG, or hot gas in the apparent cluster at  $z = 1.27$ . As seen in Figure 2, our limited optical spectroscopy does not show any significant groups along



the line of sight towards the  $z = 1.27$  galaxies, although our selection criteria for the spectroscopic observations introduces some bias into the redshift distribution. No object in the cluster field is detected down to  $\sim 20$  mJy at 327 MHz in the Westerbork Northern Sky Survey (WENSS; de Breuck, personal communication). This suggests there are no active galaxies in the SCG which could account for the observed X-ray emission. However, it is possible that an X-ray loud but radio-quiet AGN could have escaped detection by WENSS, and in fact several objects with blue  $B - R$  colors consistent with the properties of AGN lie within the SCG. But the area of interest is very small, so the likelihood of there being an AGN is very small. According to Boyle et al. (1993), we should expect to find only  $\sim 0.02$  X-ray AGN in the  $2'0$  region of the PSPC detection with  $S_\nu = 1.8 \times 10^{-14}$  ergs s $^{-1}$  cm $^{-2}$ .

The third possibility is that the PSPC detection arises from hot gas trapped in a deep potential well at  $z = 1.27$ . Assuming a gas temperature of 6 keV and a Galactic neutral hydrogen column density of  $N(\text{H}) = 2.7 \times 10^{20}$  atoms cm $^{-2}$ , the luminosity in the rest frame 0.1–2.4 keV band is  $L_x = 1.5 \times 10^{44}$  ergs s $^{-1}$  for  $h_{100} = 0.65$  and  $q_0 = 0.1$ . Although the procedure is very uncertain, we can use this  $L_x$  to estimate the cluster mass. We must assume that the gas is isothermal, that the total mass is distributed like the X-ray emitting gas, and that the gas temperature  $T_{\text{keV}}$  is related to  $L_x$  by the relationship determined at low- $z$  by Edge & Stewart (1991). Then, following Donahue et al. (1997), the total mass within a given radius  $r$  is  $M(< r) \sim 1.1 \times 10^{14} M_\odot \beta T_{\text{keV}} R_{\text{Mpc}}$ . Assuming  $\beta = 0.8$ , we find that the total mass within the Abell radius  $r = 1.5 h_{100}^{-1}$  Mpc is  $5.1 \times 10^{14} h_{100}^{-1} M_\odot$ .

The apparent confirmation of the cluster by the detection of X-ray emission from the SCG is qualified by the fact that the PSPC PSF is too broad to resolve the X-ray emission. Figure 6 shows a comparison of the growth curve of the detected X-ray source with that of a nearby star. The broader growth curve of the former is consistent with a cluster origin, but the difference is insufficient to rule out the possibility that the observed X-ray flux is due to a single galaxy, either in the apparent cluster, or along the line of sight. Nevertheless, the existence of a spatially-coincident X-ray source of a luminosity reasonable for a moderate-size cluster at  $z = 1.27$  strongly supports the identification of the SCG as a gravitationally-bound system.

#### 4. Discussion

The observations presented here provide strong evidence supporting the identification of a very red SCG found in a near-IR field survey as a galaxy cluster at  $z = 1.27$ . The density of  $J - K \gtrsim 1.9$  objects in the SCG is 5 times higher than in the rest of our Lynx survey field. The spectroscopy shows that 6 galaxies are at the same redshift within the

SCG, and another 2 more radially-distant objects are also at  $z = 1.27$ . Finally, an archival Rosat PSPC observation detects X-ray emission coincident with the SCG. The fact that no AGN are known to exist in the SCG suggests that the X-ray emission is most likely due to hot gas in the potential well of a galaxy cluster. We conclude that 0848+4453 is currently the highest redshift cluster discovered without targetting a central active galaxy.

#### 4.1. Member Galaxies

Given that we have a  $z = 1.27$  galaxy cluster, the evolutionary state of the stellar populations in the member galaxies at this substantial lookback time is of great interest. SED98 found that passively-evolving elliptical galaxies, formed at high redshift, inhabit cluster cores back to at least  $z = 0.9$ . The  $R - K$  colors of many of the objects in the cluster area show  $\sim 1$  mag of color evolution relative to our Coma-based no-evolution prediction for early-type galaxies. The  $RJK$  colors generally agree with the predictions of a passively-evolving elliptical model at  $z = 1.27$  for  $z_f > 3$  in a  $h_{100} = 0.65$ ,  $q_0 = 0.1$  cosmology. The amount of passive evolution in  $R - K$  is in good agreement with that found by SED98. The relatively blue  $B - K$  color displayed in the red objects' average s.e.d. in Figure 5 indicates there is some uncertainty in the identification of the red members as being elliptical galaxies. But Fig. 5 also shows that it takes only a very small amount of recent star formation to explain the excess flux at rest frame  $\sim 1900 \text{ \AA}$ . Most of the members in the cluster have optical spectra with the breaks and absorption lines of the evolved stellar populations seen in elliptical galaxies. The D4000 is clearly evident in 5 of the spectroscopic members, as well as B3260 and B2900 in some. A more detailed spectral analysis, akin to that in Spinrad et al. (1997) of an elliptical at  $z = 1.55$ , is deferred to a later paper.

While it is tempting to try constraining the formation epoch of the galaxies, such age estimates are very uncertain (Charlot, Worthey, & Bressan 1996), due in part to the degeneracy of age with metallicity. Also, it is difficult to distinguish between the formation of the stellar populations and the structural formation of the galaxies. Two of the cluster members, #237 and 181, are considerably bluer in  $R - K$  and  $B - K$  than the rest, and also exhibit [O II] emission. Deciding if these properties mean that these objects are late-type galaxies, or early-types with some recent star formation, is difficult without more detailed morphological information.

## 4.2. Cluster Properties

Given its high redshift, the mass of the cluster is of particular interest. Neither gravitational arcs nor weak lensing has been observed in ground-based imaging, so we cannot make use of such mass estimators. Both the  $L_x$  and the  $\sigma$  of the member galaxies indicate that 0848+4453 falls toward the low end in the mass range of low-redshift clusters (Ebeling et al. 1997; Nichol et al. 1997; Zabludoff et al. 1993). At high redshift, knowledge of the cluster distribution functions in velocity dispersion and X-ray luminosity is much poorer. Also, it is unclear if the relationships between velocity dispersion and mass, and X-ray luminosity and mass remain the same as in the present epoch. The correlation between  $L_x$  and  $\sigma$  may be shifted towards higher  $\sigma$  for a given  $L_x$ , relative to the relation at low redshift (Bower et al. 1997). In the context of CDM, one can imagine that calculations of  $\sigma$  are overestimated as a result of bound but not yet virialized galaxies, as has been suggested by the comparison of lensing mass estimates with  $L_x$  and  $\sigma$  in rich clusters at  $z \sim 0.4$  by Smail et al. (1997). The  $L_x$  and  $\sigma$  of 0848+4453 follow the low- $z$  relationship between cluster velocity dispersion and X-ray luminosity (Edge & Stewart 1991b), which may mean that the known member galaxies are virialized. On the other hand, the fact that most of the members appear to be early-type galaxies could bias the calculated dispersion. Using the CNOC sample of moderate-redshift clusters, Carlberg et al. (1997) found that the velocity dispersion of the blue members was about 30% greater than that of the red cluster galaxies. So our estimate of the dispersion may be somewhat lower than the true value for all cluster members. Also, our  $L_x$ -based mass estimate is very uncertain, given that we know very little about the physical state of the X-ray emitting gas.

If our mass estimates for 0848+4453 are approximately correct, then it is interesting to consider the resulting constraint on theories of structure and  $\Omega_0$ . The predictions of Eke, Cole, & Frenk (1996) for cluster evolution in an  $\Omega_0 = 1$  universe indicate that we should not expect to find any massive ( $M > 3.5 \times 10^{14} h_{100}^{-1} M_\odot$  according to Eke et al.) clusters at  $z > 0.5$ . The existence of 0848+4453, as well as other truly massive clusters at high redshift such as MS 1054.5-0321 (Luppino & Kaiser 1997; Donahue et al. 1997) at  $z = 0.828$ , 3C 184 at  $z = 0.996$  (Deltorn et al. 1997), and 3C 324 at  $z = 1.206$  (Dickinson 1996), indicate that  $\Omega_0 < 1$  and/or CDM is incorrect. The predicted number density of massive clusters at high- $z$  for an open universe is considerably higher (Eke, Cole, & Frenk 1996). For  $\Omega_0 = 0.3$ ,  $\Lambda_0 = 0$  there should be only 0.01 massive clusters at  $z < 1.3$  in the 100 arcmin<sup>2</sup> of the EES survey. If its mass is in fact considerably lower than our estimates based on the velocity dispersion and the  $L_x$ , then 0848+4453 could fit qualitatively, if not quantitatively, in the scenario envisioned by CDM for the growth of structure in a low  $\Omega$  universe. In this case, if we could follow it through cosmic time, we would expect to see 0848+4453 grow through mergers with other groups to become a massive cluster by the present epoch. Even more

speculatively, if we were to trace 0848+4453 back to higher redshift, we might expect to see a structure similar to the concentration of 15 Lyman break galaxies at  $z = 3.1$ , located within a  $11'$  by  $8'$  area, which were found within a  $9'$  by  $18'$  survey field by Steidel et al. (1997).

The discovery of 0848+4453 was based on the expectation that the  $J - K$  color is a reasonable redshift indicator (out to  $z \sim 2$ ) for nearly all galaxy types. This expectation has been confirmed by our finding that of the 14 galaxies with  $J - K \gtrsim 1.9$  for which spectra were obtained, 13 do indeed have  $z > 1$ . In the not too distant future near-IR imaging surveys may be able to provide large samples of  $z > 1$  clusters covering much of the cluster mass range in existence at that epoch. Such a database would prove invaluable in both the study of large-scale structure and of galaxy evolution.

We thank Ed Moran for processing the Rosat PSPC data, and Drew Phillips for the use of his slitmask software. RE and PRE thank Kitt Peak National Observatory for the support and telescope time provided to their survey. The work by SAS at LLNL was performed under the auspices of the US Department of Energy under contract W-7405-ENG-48. Extragalactic research by HS and DS is supported by NSF grant 95-28536. Portions of the research described here were carried out at the Jet Propulsion Laboratory, California Institute of Technology, under a contract with NASA. The W. M. Keck Observatory is a scientific partnership between the University of California and the California Institute of Technology, made possible by a generous gift of the W. M. Keck Foundation.

## REFERENCES

- Adelberger, K. 1996, personal communication
- Aragón-Salamanca, A., Ellis, R.S., Couch, W.J., and Carter, D., 1993, MNRAS, 248, 128.
- Bahcall, N., Fan, X., & Cen, R. 1997, ApJ, in press
- Beers, T.C., Flynn, K., & Gebhardt, K. 1990, AJ, 100, 32
- Bruzual, G. & Charlot, S. 1997, personal communication, (BC97)
- Bower, R., Lucey, J.R., & Ellis, R.S. 1992, MNRAS, 254, 589
- Bower, R., Castander, F.J., Couch, W.J., Ellis, R.S., & Böhringer, H. 1997, astro-ph/9705099
- Boyle, B.J., Griffiths, R.E., Shanks, T., Stewart, G.C. & Georgantopoulos, I. 1993, MNRAS, 260, 49
- Carlberg, R. et al. 1997, ApJ, 476, 7

- Cen, R. & Ostriker, J.P. 1994, ApJ, 429, 4
- Charlot, S., Worthey, G., & Bressan, A. 1996, ApJ, 457, 625
- Colless, M.M. 1989, MNRAS, 237, 799
- De Propriis, R., Eisenhardt, P.R.M., Stanford, S.A., & Dickinson, M. 1997, in preparation
- Deltorn, J.-M., Le Fevre, O., Crampton, D., & Dickinson, M. 1997, ApJ, 483, 21
- Dickinson, M. 1995, in *Fresh Views of Elliptical Galaxies*, A. Buzzoni, A. Renzini, & A. Serrano eds., (ASP: San Francisco), p. 283
- Dickinson, M. 1997, in *Galaxy Scaling Relations: Origins, Evolution and Applications*, L. da Costa ed., Springer-Verlag, in press.
- Donahue, M., Gioia, I., Luppino, G., Hughes, J.P., & Stocke, J. 1997, astro-ph/9707010
- Ebeling, H., Edge, A.C., Fabian, A.C., Allen, S.W., & Crawford, C.S. 1997, ApJ, 479, 101
- Edge, A.C. & Stewart, G.C. 1991b, MNRAS, 252, 428
- Eggen, O.J., Lynden-Bell, D., Sandage, A.R. 1962, ApJ, 136, 748
- Eisenhardt, P.R., De Propriis, R., Gonzales, A., Stanford, S.A., Wang, M., & Dickinson, M. 1997, in preparation
- Ellis, R.S., Smail, I., Dressler, A., Couch, W.J., Oemler, A., Butcher, H., & Sharples, R.M., 1997, ApJ, 483, 582
- Elston, R., Eisenhardt, P.R., & Stanford, S.A. 1997, in preparation, (EES)
- Eke, V.R., Cole, S., & Frenk, C.S. 1996, MNRAS, 282, 263
- Evrard, A. 1989, ApJ, 341, L71
- Fanelli, M.N., O’Connell, R.W., Burstein, D., & Wu, C.-C. 1990, ApJ, 364, 272
- Hamilton, D. 1985, ApJ, 297, 371
- Kauffmann, G. 1996, MNRAS, 281, 487
- Kinney, A., Calzetti, D., Bohlin, R.C., McQuade, K., Storchi-Bergmann, T., & Henrique, R. 1996, ApJ, 467, 38
- Lubin, L. 1996, AJ, 112, 23
- Luppino, G.A. & Kaiser, N. 1997, ApJ, 475, 20
- Nichol, R., Holden, B.P., Romer, A.K., Ulmer, M.P., Burke, D.J., & Collins, C.A. 1997, ApJ, 481, 644
- Oke, J.B. et al. 1995, PASP, 107, 3750

- Pascarelle, S.M., Windhorst, R.A., Driver, S.P., Ostrander, E.J., & Keel, W.C. 1996, ApJ, 456, 21
- Peebles, J., Daly, R., & Juskiewicz, R. 1989, ApJ, 347, 563
- Press, W.H. & Schechter, P. 1974, ApJ, 187, 425
- Smail, I., Ellis, R., Dressler, A., Couch, W.J., Oemler, A., Sharples, R.M., & Butcher, H. 1997, ApJ, 479, 70
- Spinrad, H., Dey, A., Stern, D., Dunlop, J., Peacock, J., Jimenez, R., & Windhorst, R. 1997, ApJ, 484, 581
- Stanford, S.A., Eisenhardt, P.R., & Dickinson, M. 1998, ApJ, in press. (SED98)
- Steidel, C.C., Adelberger, K.L., Dickinson, M., Giavalisco, M., Pettini, M., & Kellogg, M. 1997, ApJ, in press, astro-ph/9708125
- Valdes, F. 1982, Proc. SPIE, 331, 465
- Viana, P.P. & Liddle, A.R. 1996, MNRAS, 281, 323
- Zabludoff, A.I., Geller, M.J., Huchra, J.P., & Ramella, M. 1993, AJ, 106, 1301

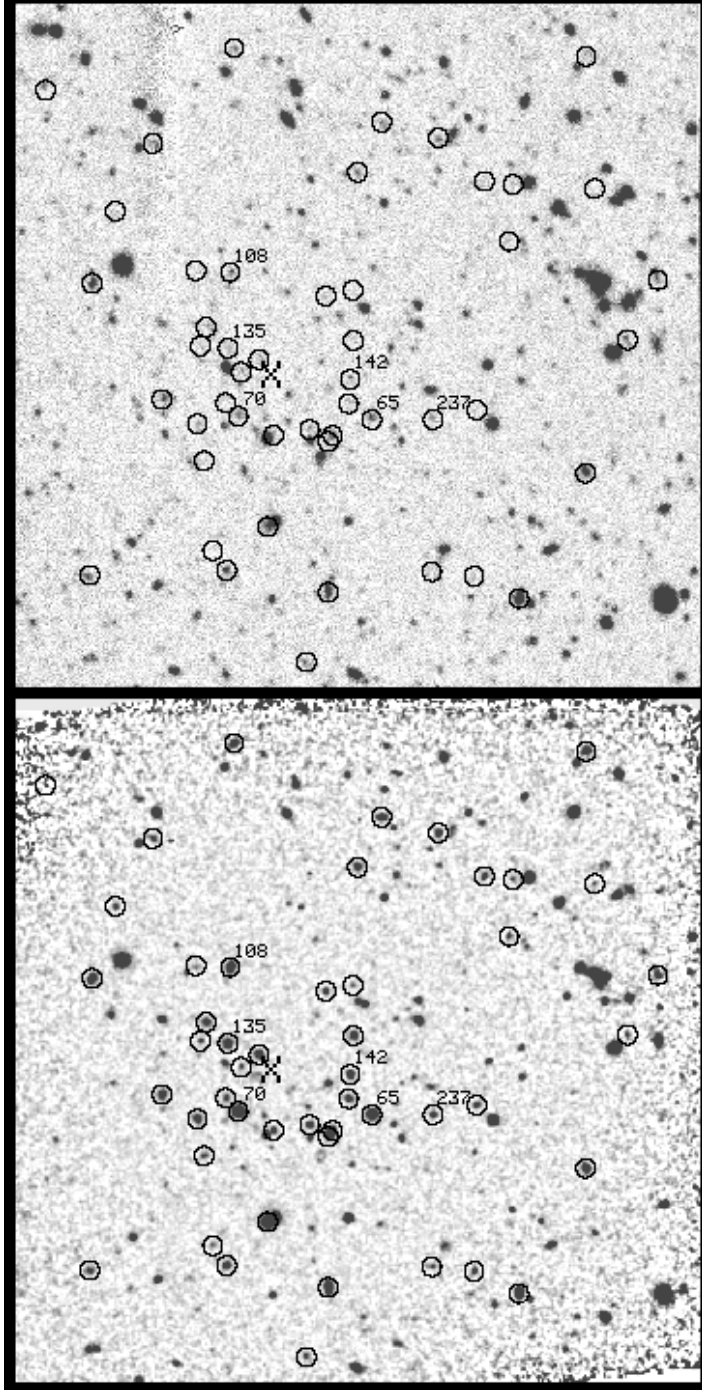


Fig. 1.—  $K$  (bottom) and  $R$  (top) band images of a  $3'.2 \times 3'.2$  area at the SCG. Objects with  $J - K \gtrsim 1.9$  are marked by the circles, and the 6 spectroscopically confirmed member galaxies within the SCG are marked with their ID numbers to the upper right. A cross marks the centroid of the PSPC detection. North is up and East is left in the images, which are centered at  $\alpha = 8^h48^m32^s.7$ ,  $\delta = +44^\circ53'56''$  (J2000).

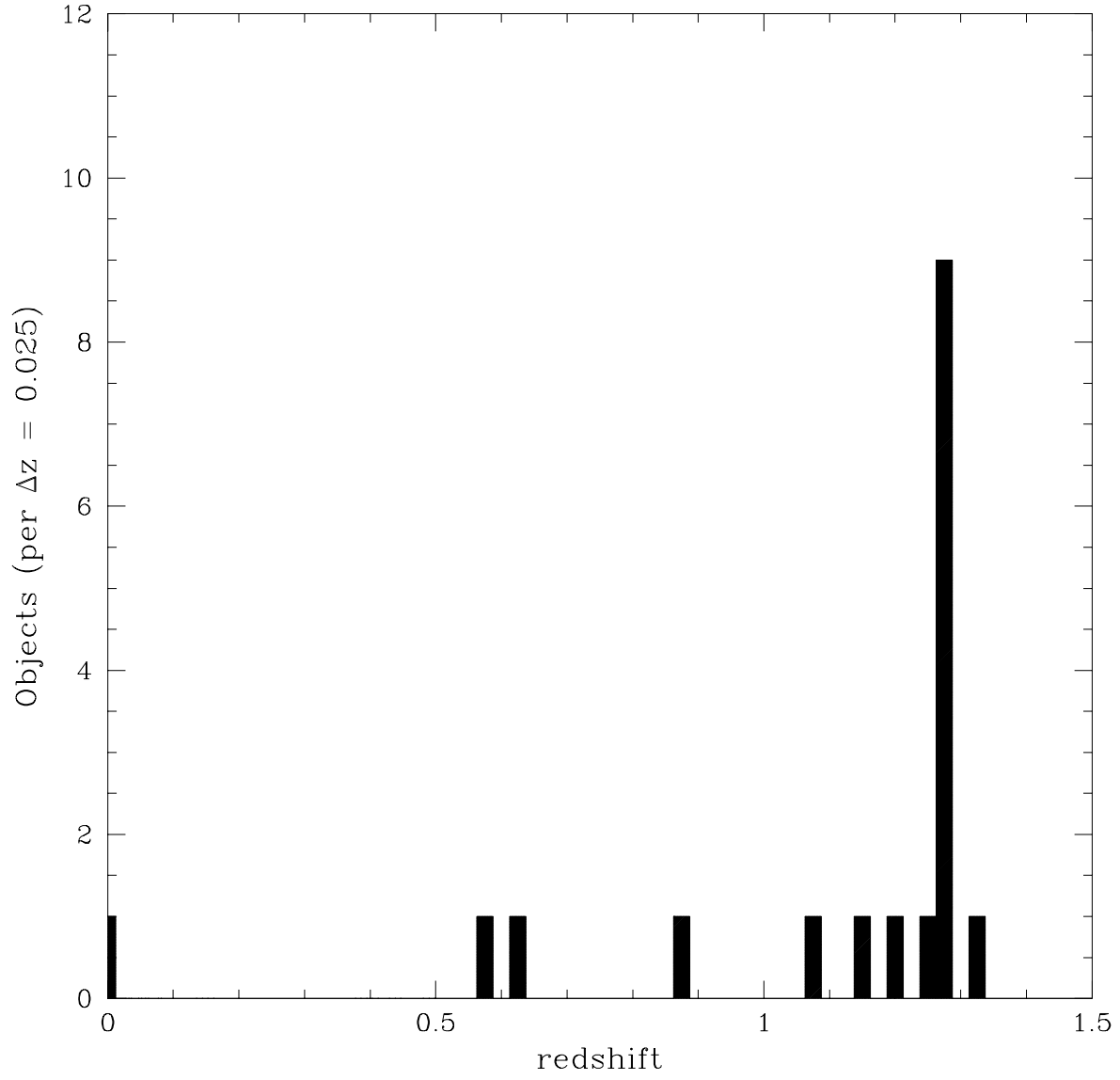


Fig. 2.— A histogram of the 18 redshifts determined in the Keck/LRIS slitmask observation.



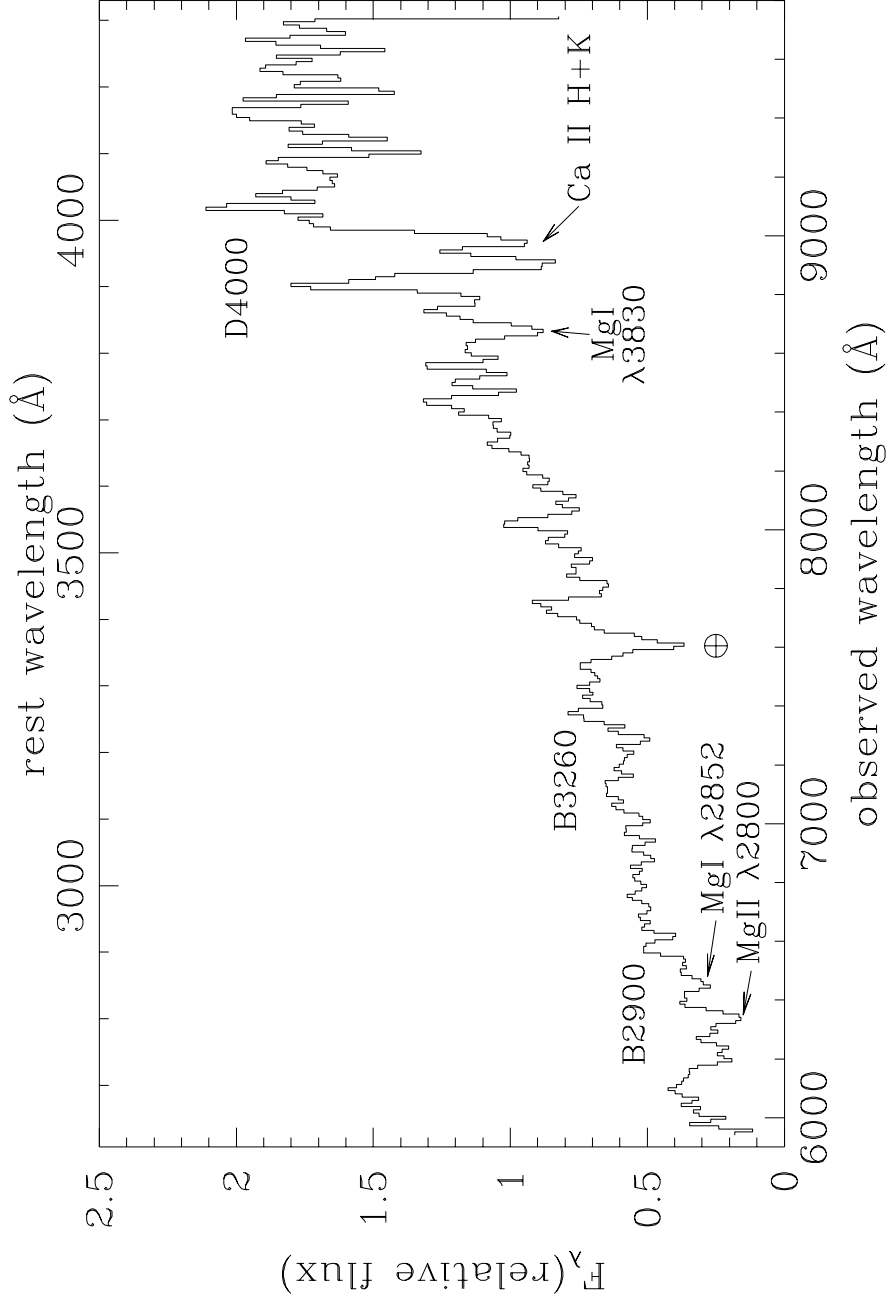


Fig. 3.— Optical spectrum of Object 65 ( $z = 1.264$ ,  $R = 24.0$ ) in ClG 0848+4453 after being smoothed by an 11 pixel boxcar.

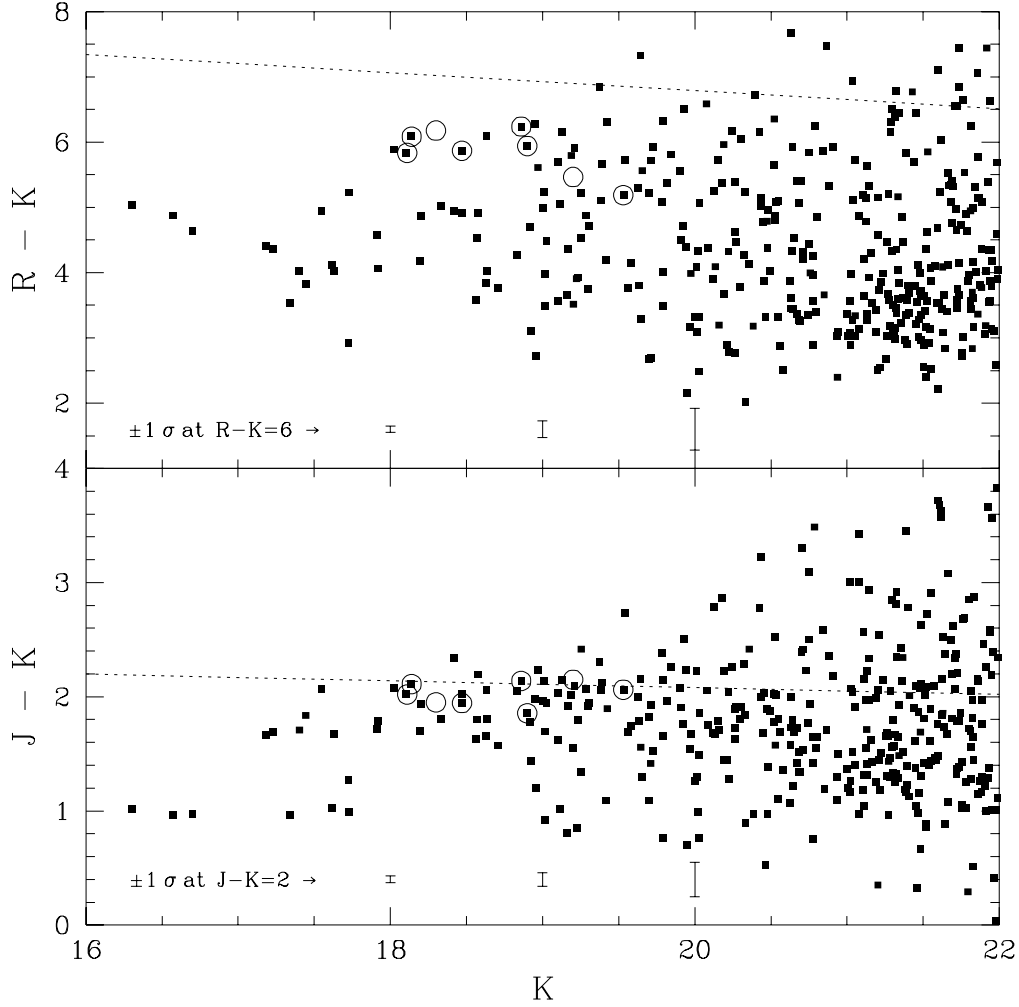


Fig. 4.— Color-magnitude diagrams of the 9 arcmin<sup>2</sup> area at the SCG. The spectroscopically identified galaxies at  $z = 1.27$  are marked with circles; note that two of these lie outside of the 9 arcmin<sup>2</sup> area (but do fall within the larger survey field) so do not appear with black squares inside. The dashed lines represent the no-evolution prediction for elliptical galaxies, as described in the text. The errors in the colors at  $J - K = 2$  and  $R - K = 6$  are shown at the bottom of the panels.

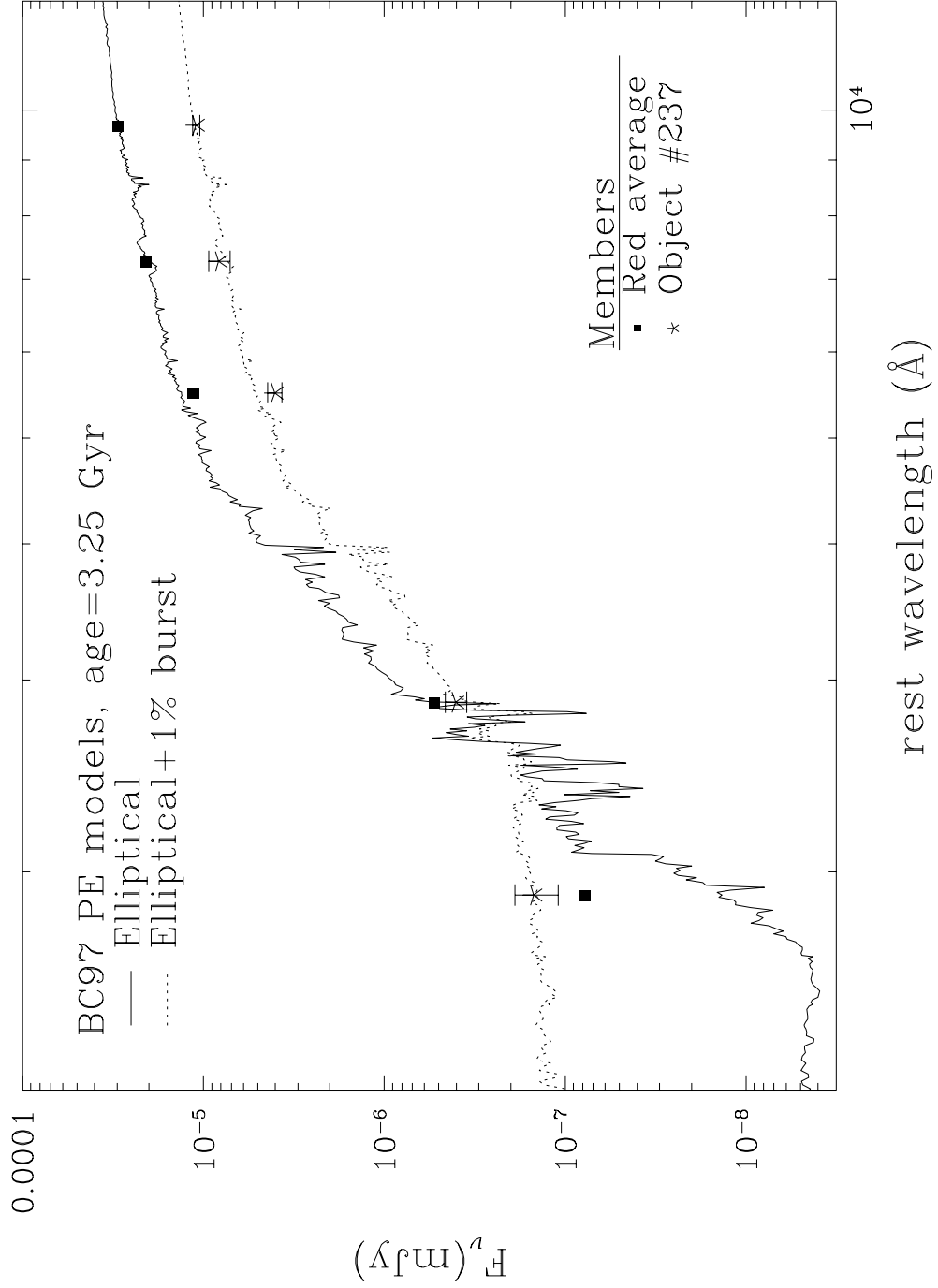


Fig. 5.— Rest frame spectral energy distributions of the spectroscopic members. The solid squares represent the average of the 5 red galaxies within the SCG, and the open stars (with  $\pm 1 \sigma$  errorbars) represent #237. The two spectra plotted in the figure were generated from BC97 passive evolution models, and are described fully in the text.

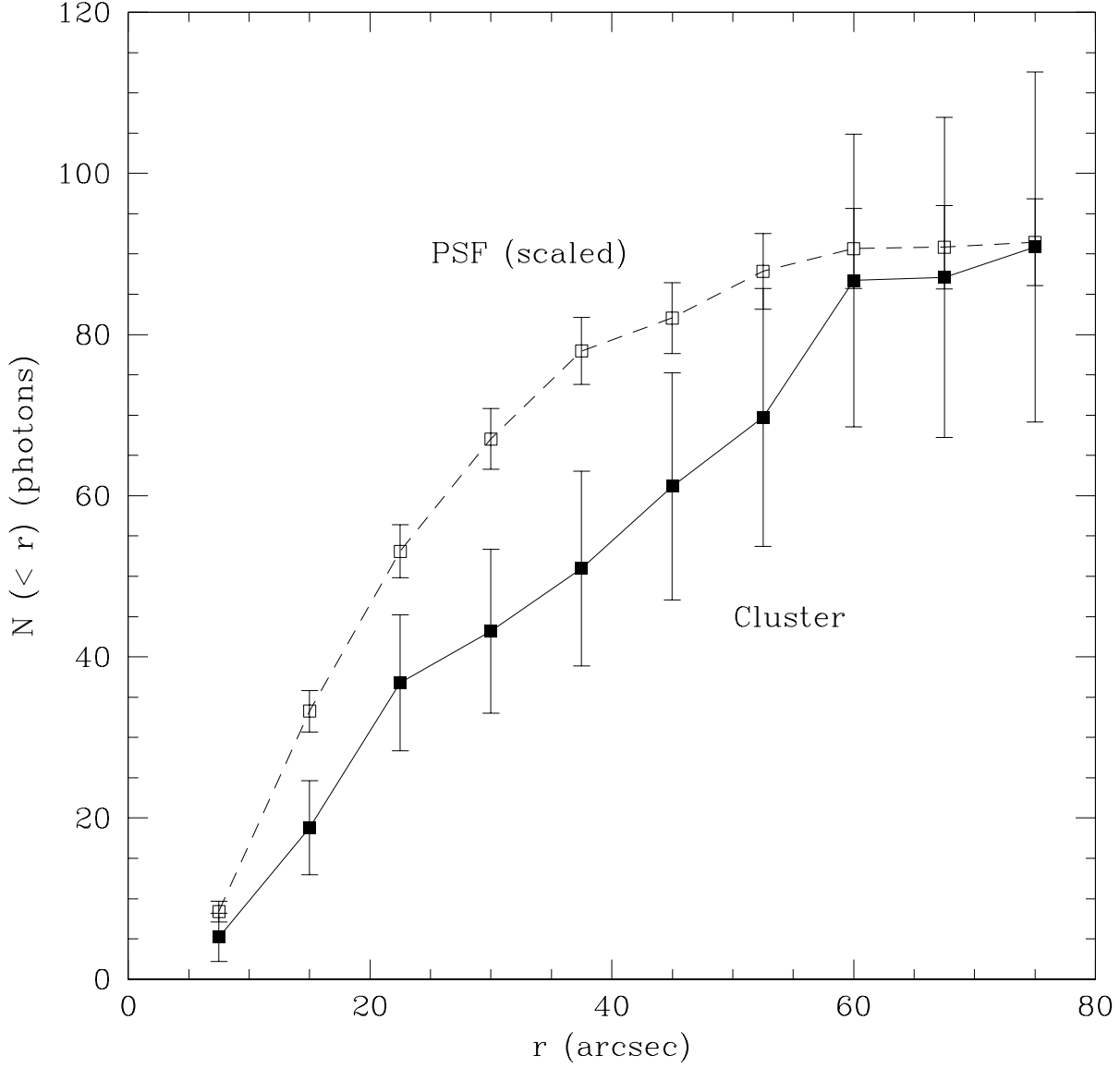


Fig. 6.— The Rosat/PSPC growth curve of a nearby star compared to that of the X-ray source at 0848+4453.  $\pm 1\sigma$  error bars are shown. The nominal FWHM of PSPC data within the on-axis field is  $\approx 23$  arcsec; the cluster is unresolved within the errors.

Table 1. Summary of Spectroscopic Targets in Lynx Field

ID	R.A.	Dec.	$z$	$J - K$	$R$	Radius <sup>a</sup>
237	08:48:30.73	44:53:36	1.271	2.1	24.7	37
65	08:48:32.36	44:53:36	1.263	2.0	24.0	19
142	08:48:32.92	44:53:47	1.277	1.9	24.8	18
70	08:48:35.93	44:53:37	1.275	2.1	24.2	20
135	08:48:36.18	44:53:56	1.276	2.1	25.1	22
108	08:48:36.06	44:54:18	1.277	1.9	24.4	45
95	08:48:32.51	44:51:41	1.268	1.9	24.4	129
181	08:48:45.54	44:54:31	1.270	2.1	24.7	136
207	08:48:43.97	44:53:11	1.065	1.9	25.0	107
262	08:48:41.98	44:55:02	...	1.3	25.4	122
167	08:48:46.80	44:55:01	1.24	1.9	24.3	162
200	08:48:53.24	44:53:49	0.875	1.7	23.9	277
162	08:48:50.21	44:55:10	1.138	1.9	24.5	199
118	08:48:50.84	44:55:34	1.328	1.9	24.5	217
148	08:48:52.92	44:55:21	1.273	1.8	24.3	230
109	08:48:52.65	44:56:13	0 <sup>b</sup>	0.8	23.3	206
305	08:48:56.28	44:55:51	1.21	1.9	24.9	276
82	08:48:57.56	44:56:11	0.622	1.9	23.1	299
55	08:48:57.06	44:56:48	0.569	1.6	22.8	310

<sup>a</sup>Radius is the distance in arcsec from the SCG center

<sup>b</sup>M star

Note. — Coordinates are J2000

Table 2. Spectroscopic Results for Members in ClG J0848+4453

ID	$z$	$\delta z$	Major Spectral Features
65	1.2637	0.0003	H+K, MgII $\lambda$ 2800, D4000, B3260, B2900
70	1.2751	0.0004	H+K, MgII $\lambda$ 2800, D4000, B2900, wk. [O II]
108	1.2783	0.0003	H+K, MgII $\lambda$ 2800, D4000, B2900, B2640, wk. [O II]
95	1.2678	0.0005	H+K, D4000, G-band
135	1.2758	0.0006	H+K, D4000
142	1.2789	0.0003	H+K, MgII $\lambda$ 2800, D4000, B2900, B2640
181	1.2706	0.0002	[O II], MgII $\lambda$ 2800, D4000, H $\delta$ , G-band
237	1.2714	0.0002	[O II], MgII $\lambda$ 2800, H $\delta$ , H+K

Table 3. Photometric Properties of Members in ClG J0848+4453

ID	$K$	$H - K$	$J - K$	$R - K$	$B - K$	$M_V^a$
65	$18.11 \pm 0.02$	$0.81 \pm 0.03$	$2.02 \pm 0.03$	$5.86 \pm 0.05$	$8.6 \pm 0.2$	$-23.4$
70	$18.14 \pm 0.02$	$1.00 \pm 0.03$	$2.11 \pm 0.03$	$6.09 \pm 0.05$	$8.7 \pm 0.2$	$-23.5$
95	$18.30 \pm 0.02$	$\dots$	$1.95 \pm 0.04$	$6.18 \pm 0.07$	$8.7 \pm 0.2$	$-23.0$
108	$18.47 \pm 0.02$	$0.89 \pm 0.04$	$1.94 \pm 0.04$	$5.87 \pm 0.06$	$8.6 \pm 0.2$	$-23.1$
135	$18.86 \pm 0.03$	$1.09 \pm 0.05$	$2.13 \pm 0.05$	$6.24 \pm 0.11$	$8.5 \pm 0.3$	$-22.5$
142	$18.90 \pm 0.03$	$0.84 \pm 0.05$	$1.87 \pm 0.06$	$5.94 \pm 0.09$	$8.5 \pm 0.3$	$-22.4$
181	$19.20 \pm 0.05$	$\dots$	$2.15 \pm 0.10$	$5.47 \pm 0.09$	$7.4 \pm 0.2$	$-21.9$
237	$19.53 \pm 0.06$	$0.83 \pm 0.09$	$2.06 \pm 0.12$	$5.19 \pm 0.10$	$6.8 \pm 0.1$	$-21.7$

<sup>a</sup>Calculation of  $M_V$  assumed  $h_{100} = 0.65$ ,  $q_0 = 0.1$ ; see text for details.